



Optical deflection measuring system

Miha Vrhovec^{a,*}, Igor Kovač^b, Marko Munih^a

^a Faculty of Electrical Engineering, University of Ljubljana, Tržaška c. 25, 1000 Ljubljana, Slovenia

^b Institute of Production Engineering, Graz University of Technology, Kopernikusgasse 24, A-8010 Graz, Austria

Received 15 February 2006; received in revised form 5 June 2006; accepted 21 June 2006

Abstract

A system for accurate real-time measurement of deflections was developed. A stable laser source is, by means of a single-mode fiber, coupled to an optical head located at one end of deformed structure. A detector circuit with a quadrant detector and processing electronics, located at the other end of the structure, communicates the resolved 2D position of the incident beam over a common digital bus. Experiments using interferometers were conducted in a climate-controlled chamber to evaluate system performance and verify the accuracy. A resolution of 0.1 μm is attainable in dynamic measurements. The system was calibrated and tested to yield measurement accuracy of $\pm 0.8 \mu\text{m}$ for $\pm 2\sigma$ probability over the measurement range of $\pm 300 \mu\text{m}$. Drift of the system in the experimental setup was determined to be less than 2 μm for measurement in both degrees of freedom within the 10 h period under constant environmental conditions.

© 2006 Published by Elsevier Inc.

Keywords: Optical deflection measuring; Real-time error compensation; Laser deformation measurement

1. Introduction

Optical methods have been used in various fields of science and industry in order to detect small deviations in position or angle. These systems often employ a laser source, producing an optical reference line, and a kind of position sensitive detector (PSD) to measure the deviation from the reference line. Different types of PSDs include segmented photodiodes, lateral-effect photodiodes and CCD detectors, among others. An autocollimator, e.g. such as described by Sohn et al. [1], uses a laser diode, PSD and a moving mirror to detect small changes in angle of the mirror. Armstrong and Fitzgerald [2] proposed an autocollimator comprising a CD player pick-up head and a reflecting surface. The head contains a laser source and photodiodes that can be used to establish the reflected beam deflection. Likewise, Fan et al. [3] used a DVD player head and a knife-edge principle in a straightness measuring system.

Similar systems were also used to measure geometrical errors of precision machinery, such as machine tools, coordinate measuring machines (CMMs) and others. When high accuracy is required, two different approaches can be used. First, errors

can be avoided with a proper design of the machine by means of a rigid construction and close manufacturing tolerances. Second, they can be compensated for in real-time during machine operation. The latter method was found to be more cost effective than the traditional error avoidance approach and has been under constant development in recent years. Error compensation includes two different concepts, namely the off-line and on-line compensation. Off-line methods can improve the accuracy by applying either mathematical models of errors or previously established calibration data. Although effective only to a certain extent, calibration techniques were shown to significantly improve the accuracy [4].

Random non-repeatable errors caused by machine load, friction, environmental and other sources can, however, only be overcome by measuring and compensating them in real-time. Huang and Ni [5] presented an error compensation system for CMMs with a five DOF measuring system for X and Y-axes and a two DOF measuring system for Z-axis of the machine. The first unit contains a He–Ne laser, optical components to generate four separate beams and PSDs to measure vertical and horizontal straightness, roll, pitch and yaw errors. The Z-axis unit measures only the straightness errors due to space and weight limitations. Additional PSDs were used to compensate the lateral drift of the laser beam. The achieved accuracy of the system was 1'' for angle and 5 μm for translational errors. The

* Corresponding author. Tel.: +386 1 4768742; fax: +386 1 4768 239.
E-mail address: miha.vrhovec@robo.fe.uni-lj.si (M. Vrhovec).

64 problem of beam stability was addressed by Fan and Zhao in [7].
65 He used a fiber-coupled laser and a modulation circuit in order
66 to diminish the lateral and angular beam drift. The resulting
67 system stability was $0.3 \mu\text{m}$ at 1 m distance in 12 h period and
68 the accuracy was $0.3 \mu\text{m}$ within $\pm 100 \mu\text{m}$ range. Feng [6] also
69 used a laser coupled to a single-mode optical fiber in straightness
70 measurement system. The obtained repeatability was $1 \mu\text{m}$ at
71 1 m distance and the drift was $3 \mu\text{m}$ in 10 min period. Recently,
72 Kuang et al. [8] introduced a four DOF measurement system
73 with a fiber-coupled laser with an accuracy of the straightness
74 part of $\pm 2.5 \mu\text{m}$ and stability of $1.4 \mu\text{m}$ in 1 h interval.

75 In robotics, such systems were proposed to measure the def-
76 lections of a flexible robot structure. With lightweight manipu-
77 lators, the assumption of rigid links is usually not valid. The ex-
78 istence of deflections and vibrations makes the measurement of
79 the link deformations necessary. Attempts to measure defor-
80 mations indirectly have been made, using strain gauges, fibre-optic
81 and other sensors. Actual deflections are then inferred from these
82 partial strain information by complex operations, which are of-
83 ten noisy and inaccurate. In this respect, optical methods are
84 advantageous by measuring the deflections directly. Demeester
85 and Van Brussel [10] presented a sensor system consisting of
86 three laser diodes and three PSDs, mounted on opposite sides
87 of a flexible link. Five components of total six DOF deflection
88 are measured, excepting the elongation of the link. Xu and
89 Tso [11] proposed an optical sensing system for measuring five
90 DOF deflection of each flexible link and a compensation scheme
91 to improve robot positioning accuracy. Yang [12] considered a
92 simplified system, measuring only errors in the nominal motion
93 plane, perpendicular to preceding joint axis. Tso et al. [13]
94 demonstrated vibration control of a single flexible link by using
95 a one-axis optical feedback system.

96 All previously mentioned optical systems have shown to sig-
97 nificantly improve the accuracy of the mechanical structure.
98 Nevertheless, they lack physical attributes (weight, dimension)
99 or accuracy properties much needed for use in real machinery.
100 Externally mounted sensitive components cannot be exposed to
101 the industrial environment and may in different ways obstruct the
102 operation of the machine. Moreover, an effective way to capture
103 deflection data from multiple such systems is desired. In this pa-
104 per, we present a solution with capability of static and dynamic
105 measurement of deflections, developed for integration in preci-
106 sion mechanical systems at the University of Ljubljana. Simp-
107 licity, high accuracy and easy practical implementation were
108 desired prime objectives. The system is distinctive for its small
109 weight and compact dimensions, making it possible to locate it
110 internal to a machine segment, robot or other structure. In this
111 way, the normal functionality of the machine is unimpeded and
112 at the same time, favorable operating conditions for the optical
113 system can be attained.

114 **2. Deflection measurement system**

115 *2.1. Measurement principle*

116 In Fig. 1, a single link of a flexible structure is shown. The
117 coordinate frame O_0 is placed at one end of the link and coin-

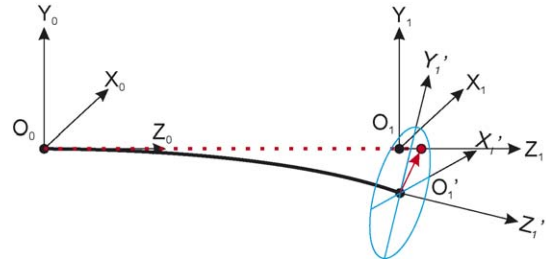


Fig. 1. A deformed link.

118 cides with an optical head producing a straight reference beam.
119 At the other end of the link, a detector circuit establishes the
120 position of the projected light spot in the O_1' coordinate frame.
121 The deflection from the straight line can be represented by a
122 transformation from coordinate frame O_1 to O_1' . Since the error
123 components in Z-direction (the elongation of the link) are
124 usually very small, they can be neglected [11] within defined
125 temperature conditions. By using a single reference beam and
126 a quadrant detector, the linear displacements in the plane per-
127 pendicular to the beam (X and Y translational errors) can be
128 measured. Often, the rotations around X- and Y-axes can also
129 be inferred from this information, e.g. when only gravitational
130 loads are present, or by assuming the dominant mode shapes in
131 oscillating structures [13]. Therefore, at most four of total six
132 components of deviation can be identified.

133 When the segment is undisturbed, the reference beam hits the
134 center of the photodiode, producing equal output in each of the
135 quadrants. Any deviation of the detector in the plane perpen-
136 dicular to the beam causes a displacement of the light spot (Fig. 2).
137 The maximum deviation from the center position is limited by
138 the spot diameter and is usually $< 0.9r$. A simple measure of
139 the displacement can be found as:

$$dX' = \alpha \frac{(V_B + V_C) - (V_A + V_D)}{V_A + V_B + V_C + V_D} \quad (1) \quad 140$$

$$dY' = \alpha \frac{(V_A + V_B) - (V_C + V_D)}{V_A + V_B + V_C + V_D} \quad (2) \quad 141$$

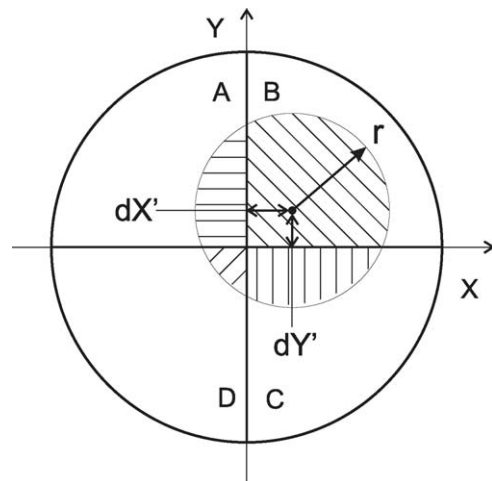


Fig. 2. A quadrant photodiode and an incident beam.

142 where V_A , V_B , V_C and V_D are the voltages proportional to illumination of respective photodiode quadrants and α is proportional
143 to the beam diameter. These equations are exact only in case
144 of a perfectly rectangular beam with a uniform intensity distribution.
145 In reality, however, the circular shape and the beam intensity
146 distribution cause significant non-linear deviations from these idealized equations, as it was discussed in [9]. The beam
147 diameter also influences the resolution of the measurement. A
148 complete theoretical characterization of the displacement curve
149 is difficult because of the Bessel distribution of the beam [6] and
150 has only limited applicability on account of beam irregularities,
151 caused by lens and scattered light. An experimental calibration
152 is therefore necessary.

155 The plane of the PSD is expected to be normal to the laser
156 beam. Nevertheless, the bending of the link will cause an angular
157 deviation of the link and the PSD plane. This will introduce
158 a cosine error in the measurement and effectively change the
159 sensitivity of the detector to the lateral movement, since it is now
160 inclined with regard to the reference beam. But the extent of this
161 sensitivity variation is in most cases very small. If we assume
162 a uniform profile of the link, the Eqs. (3) and (4) describe the
163 lateral and angular deflections of the link under point load at the
164 end of the link, respectively [14]:

$$165 \quad f = \frac{Fl^3}{3EI_Y} \quad (3)$$

$$166 \quad \alpha = \frac{Fl^2}{2EI_Y} \quad (4)$$

167 Here, f and α denote the lateral and angular deflections, F the
168 applied force, l the length of the link and I_Y is the area moment
169 of the link cross-section. The relation between the two is
170 therefore:

$$171 \quad \frac{\alpha}{f} = \frac{3}{2l}. \quad (5)$$

172 The equation demonstrates that the ratio of angular to the lateral
173 deflection is inversely proportional to the link length. Similar
174 relation can be found for a load distributed along the link (e.g.
175 gravity load). At link lengths, greater than 30 mm, the sensitivity
176 change results in less than 0.01% reading deviation, so this effect
177 can be neglected.

178 2.2. System components and operation

179 The main components of the system are presented in Fig. 3.
180 The laser control unit drives the laser diode producing a visible
181 output wavelength of 670 nm. A feedback circuit provides a
182 constant optical power output of the laser diode, which is coupled
183 to a single-mode optical fiber. This is known to reduce the lateral
184 and angular drift of the beam common to laser diodes. The beam
185 emanating from a single-mode fiber has a constant, Bessel distribution
186 and does not suffer from any spatial drift. The optical fiber is
187 terminated by an optical head containing a lens system. It collimates
188 the light emerging from the fiber, producing a beam with an approximate
189 diameter of 1 mm and 0.5 mrad divergence. Through usage of an
190 optical fiber and stable laser

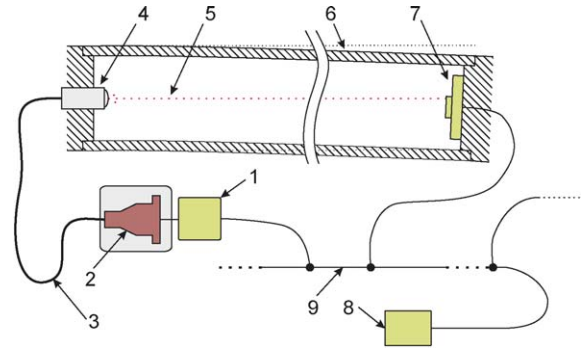


Fig. 3. Main system components: (1) laser driving unit, (2) laser diode, (3) optical fiber, (4) optical head, (5) reference beam, (6) deflected link, (7) detector circuit, (8) master circuit, and (9) digital bus.

191 driver components [6,8], a high-quality reference beam of an
192 adequate stability is generated.

193 The detector circuit board is placed at the other end of the
194 measured segment. A schematic diagram of the detector assembly
195 is shown in Fig. 4. The incident beam hits the quadrant photo-
196 diode, consequently generating four photocurrents, proportional
197 to optical power over each quadrant. These small currents are
198 then amplified and converted to voltages, to be added and sub-
199 tracted as per Eqs. (1) and (2). A 16-bit ADC digitizes the values,
200 which are processed and stored by an onboard microcontroller.
201 The quantization step (1 LSB) of the A/D conversion in the cur-
202 rent system corresponds to approximately 0.01 μm resolution.

203 The distinct advantages of this measurement device are its
204 small size and low weight. Since the optical head is separated
205 from the laser source by the optical fiber, its dimensions can be
206 kept very small. This also has an additional advantage of dislo-
207 cating the heat source from critical mechanical components. The
208 compactness of the detector was achieved by developing small
209 size electronic boards. Merely the components needed for the
210 purpose were included and space efficient surface-mount tech-
211 nology was utilized. The components are located on two stacked
212 boards, which were size-optimized to meet the dimensions as
213 specified in Table 1. The finished prototypes of the optical head
214 and the detector unit are pictured in Fig. 5. Because both main
215 parts of the system, the optical head and the detector unit, are of
216 small physical dimensions, they can be completely contained in
217 the measured segment. The entire optical path of the reference
218 beam is then held in an enclosed space with stable environmental
219 parameters, therefore some disturbing factors that affect similar
220 systems, namely the ambient lightning and air turbulence, can
221 now be minimized. Two example applications of the system are
222 shown on Fig. 6.

223 A multitude of such detector units can be connected to a dig-
224 ital bus, all communicating with a single master unit. The exact
225 moment when the deflection data is converted and stored can be
226 defined by asserting the common trigger signal, thus synchron-
227 izing the measurement of all detector units. Alternatively, the
228 measurement can be software triggered by an external controller
229 or the detected position can be continuously output with the
230 maximum sample rate. The master board contains the hardware
231 facilities and protocols to transfer all deflection and control data
232 to an external controller or computer. At this stage it is equipped

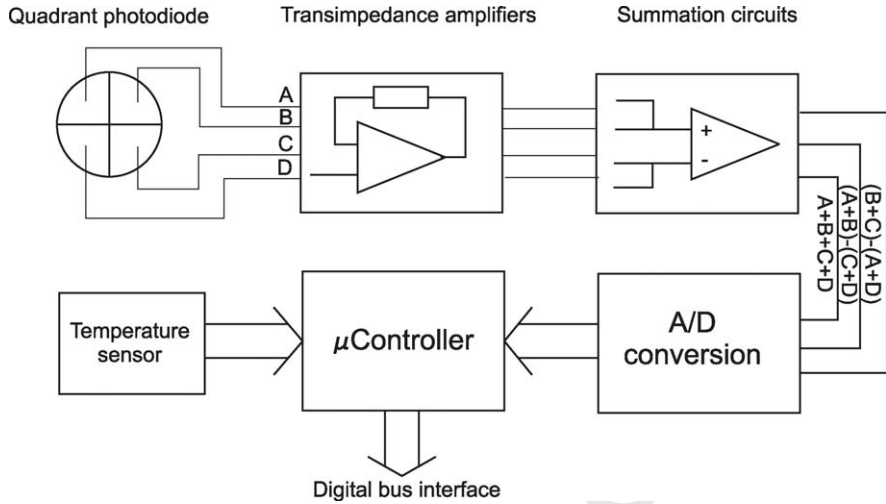


Fig. 4. Detector circuit board components.

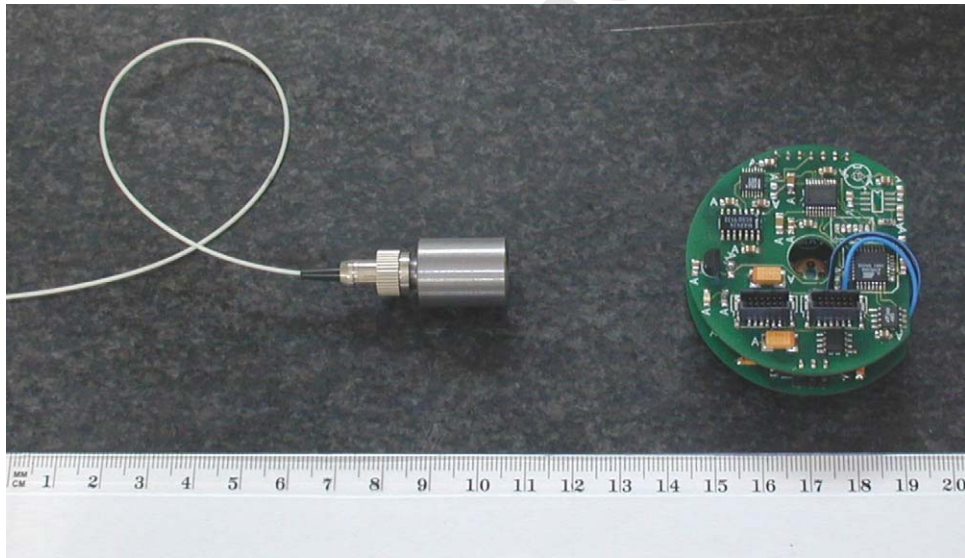


Fig. 5. The finished optical head and detector components.

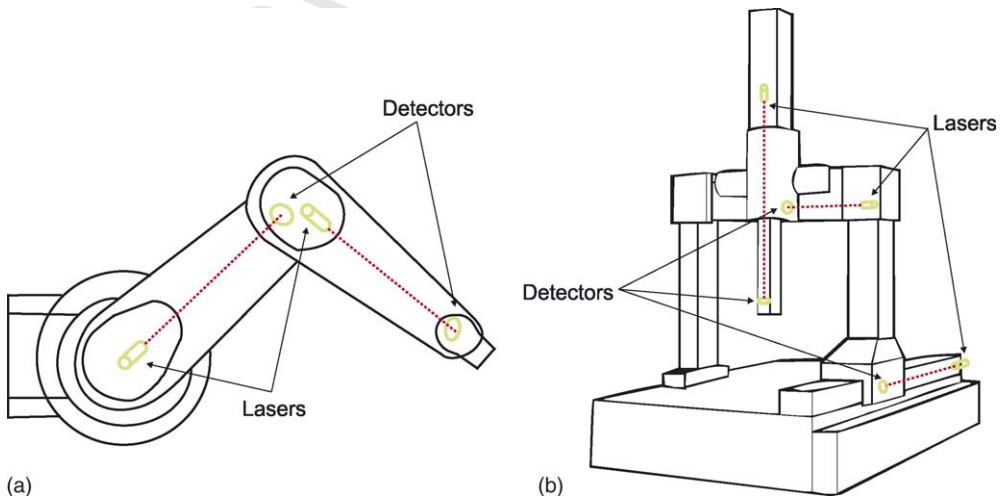


Fig. 6. Example applications of the measuring system: (a) in a robot and (b) in a CMM.

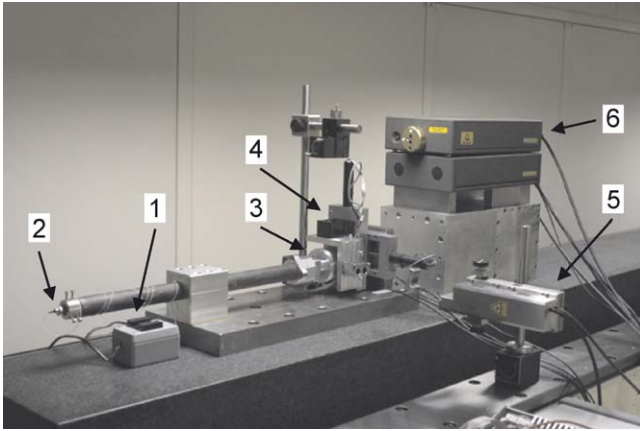


Fig. 7. Experimental system setup: (1) laser unit, (2) optical head, (3) detector, (4) micropositioning stages, (5) X-axis interferometer, and (6) Y-axis interferometer.

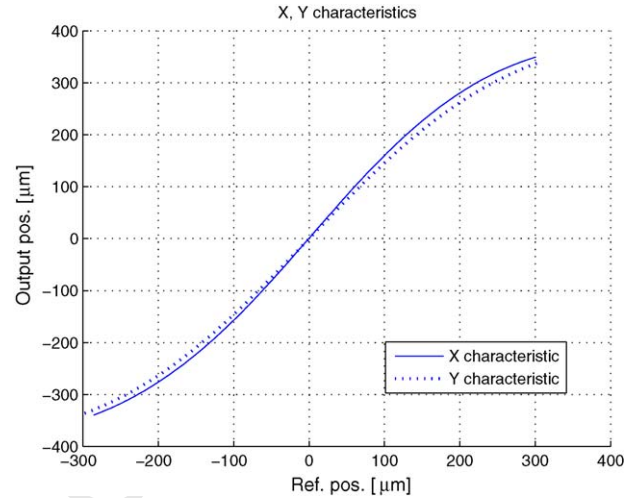


Fig. 8. X and Y detector response.

233 with an USB interface, enabling the system to be connected to
234 any personal computer and capture data with a 1.2 kHz sampling
235 frequency.

236 3. Experiments

237 3.1. Experimental setup

238 To characterize, calibrate and validate the new measurement
239 system as proposed in Sections 2.1 and 2.2, an experimental
240 setup as pictured in Fig. 7 was employed. The optical head
241 was fastened to one end of a 0.6 m long carbon-fiber tube having
242 23 and 30 mm outer diameter, respectively. The practical im-
243 plication of the tube was to contain the laser beam in stable
244 (non-turbulent) environment and was not actively deformed. In-
245 stead, the detector was moved in the measuring plane by means

of two Physik-Instrumente M-150.10 micropositioning stages, 246
arranged in a X–Y configuration. The measured resolution of the 247
stages was approximately 0.2 μm and the bidirectional repeatability 248
2 μm. The detector was contained in aluminium housing and fastened 249
to the positioning stages, which were, in turn, fixed to the base 250
steel plate together with the tube and optical head. The whole setup 251
was then rested on a massive granite table, providing a stable and 252
vibration-free support. 253

To accurately measure the actual relative position of the 254
detector, two laser interferometer systems were used. The hori- 255
zontal movement was measured by the Heidenhain ILM-1131 256
interferometer and the vertical by Renishaw ML10 + EC10 system. 257
The stated resolutions of the reference measuring systems were 0.1 258
and 1 nm, respectively. In the laboratory environment, the accuracy 259
of these systems is 0.1 μm, which was sufficient for the intended 260
experiments. The retroreflectors were rigidly 261

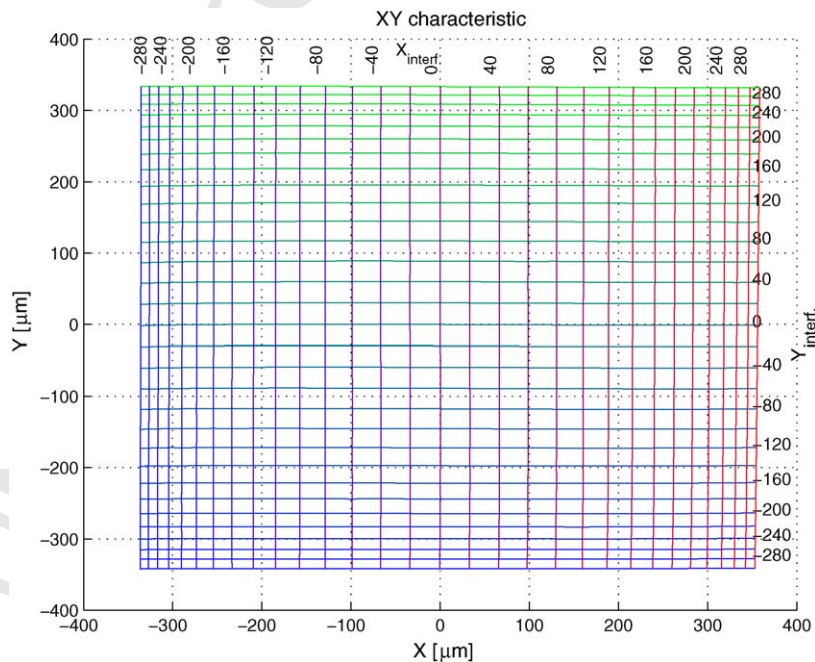


Fig. 9. 2D detector response.

mounted to the detector housing in the axes of quadrant photodetector in order to minimize errors caused by angular deviations of positioning stages.

The measuring setup was located in a climate-controlled chamber [15] at the Institute of Production Engineering, TU Graz, to avoid temperature induced deformations of the critical elements. A desktop PC was used to control the positioning stages and retrieve the captured data from deflection measurement system and both interferometers. A common trigger signal was used for exact synchronization of all measuring systems. At the same time, the temperature values of the surrounding air and the steel base were also acquired. A PC application for unattended execution and control of measuring sequences was developed, creating an automated calibration and test system. Therefore, it was possible to avoid any possible external disturbance to the measurements.

3.2. Results and discussion

The purpose of the experiments was to assess basic system characteristics, calibrate it and evaluate its accuracy properties. First, one-dimensional response curves of the detector were recorded (Fig. 8). Detector response in X-direction was measured with Y-axis in center position and for Y-direction with X-axis in center position. The curves were found concordant with theoretical predictions. With increasing distance from central region with good linearity, the sensitivity is falling because of circular beam shape and its distribution. The slight difference in sensitivity of X- and Y-axis originates from beam ovalness and deviations in analog electronics. Unwanted properties such as hysteresis and dead-zone were below the limit of detection. The position resolution of the system depends on well definable and measurable factors, such as electronic noise and A/D conversion resolution as well as on random circumstances, such as thermal conditions and air turbulence in the light path. The former amounts to less than $0.05 \mu\text{m}$ and the overall resolution was experimentally verified to be $0.1 \mu\text{m}$ in conditions, as specified in Section 3.1. In static measurements, the resolution can be increased by time averaging techniques.

Next, a 2D characteristic was measured (Fig. 9). Because of the above mentioned small irregularities in beam distribution and analog electronics, the response curves in X-axis direction depend on Y-axis coordinate and vice versa. For this reason, a 2D response calibration is necessary for accurate results. The procedure for acquiring Fig. 9 was as follows. The response curves of the detector in X-direction were recorded and the Y position was then shifted for $20 \mu\text{m}$ repeatedly across the measurement range in order to obtain the horizontal lines. The same was done with Y-axis for the vertical lines. The resulting curves in Fig. 9 are plotted in uncalibrated space, according to Eqs. (1) and (2). The X- and Y-axes represent the detector output coordinates and the plotted horizontal and vertical arrays correspond to actual positions as measured by the interferometers. It is evident that the sensitivity is falling with increasing distance from the center point. With the measurement range chosen as $-300 \mu\text{m} < X, Y < 300 \mu\text{m}$, the sensitivity on the edge is about one-third of maximum (center) sensitivity.

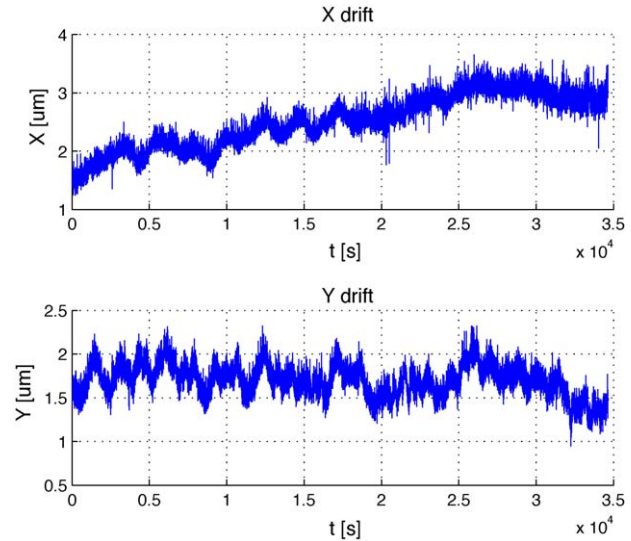


Fig. 10. Position drift of the system.

The system drift was also measured. In a thermally stable environment, the position was measured for a period of 10 h with 1 Hz sampling frequency. The positioning stages were left fixed in approximate center position of the detector. The results, shown in Fig. 10, indicate position reading drift of less than $2 \mu\text{m}$ for X-axis and $1 \mu\text{m}$ for Y-axis in the stated interval of 10 h. The likely sources of positional drift are mechanical deformations caused by the remaining temperature changes and small spatial deviations of the laser beam. The drift quantified here does not prevent higher degree of accuracy in shorter period of time. Successive calibrations, if possible, could bring the short term stability within $0.5 \mu\text{m}$ over 30 min time interval.

Finally, the system accuracy was tested. The data acquired for 2D characteristics presented in Fig. 9 was used to calibrate the system, after which the detector was moved into 400 random positions, uniformly distributed in the measuring range. The position output from our detector was calculated using 2D interpolation of the calibration data, and the true positions were measured simultaneously by the interferometers as reference values. The resulting positional deviations of successive measurements are in Fig. 11. It can be seen that the maximum error after detector calibration was $1.3 \mu\text{m}$ for the X-axis and $1 \mu\text{m}$ for the Y-axis. Slightly better agreement of the measured and reference position is visible in the Y-axis results. Also, small drift is present in X-axis position, since the duration of measurement was more than 30 min. The statistical distribution of the errors is in Fig. 12. As expected, the shape of the distribution is close to Gaussian (dashed line in the graphs). The standard deviations of the error data for X- and Y-axes amount to $\sigma_X = 0.4$ and $\sigma_Y = 0.35$, respectively. We can therefore expect with approximately 95% ($\pm 2\sigma$) certainty the measurement result is within $\pm 0.8 \mu\text{m}$ of the true value. These values could be further improved by applying better calibration and position estimation methods, e.g. spline instead of linear interpolation. Again, accuracy can be further enhanced in static or quasi-static conditions by averaging the measurements in a sufficient time interval.

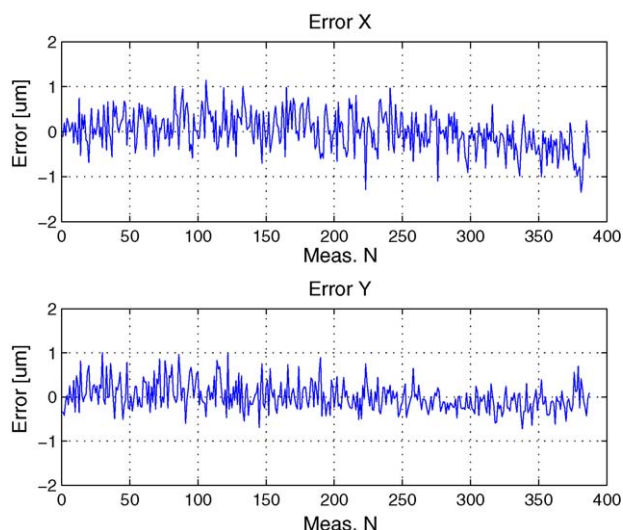


Fig. 11. Measurement error in test points.

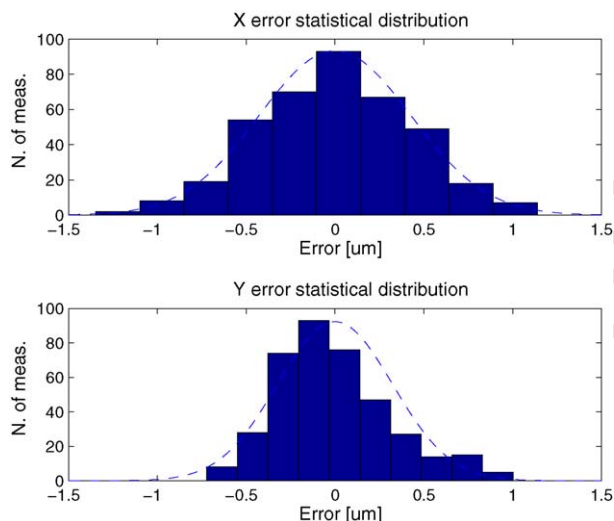


Fig. 12. Statistical distribution of measurement error.

The accuracy alleged here applies to the specific detector unit in the calibration setup. The misalignment of the PSD relative to the detector mounting has been taken into account by the calibration procedure. However, care must be taken when positioning the detector unit into the target system. The out-of-plane rotation of the unit will cause an observable cosine error if the mounting error is greater than 1.5° . Likewise, the in-plane ro-

Table 1
System characteristics

Range	X, $\pm 300 \mu\text{m}$; Y, $\pm 300 \mu\text{m}$
Resolution	$0.1 \mu\text{m}$
Accuracy ($\pm 2\sigma$)	$\pm 0.8 \mu\text{m}$
Maximum sample rate	1.2 kHz
Trigger response time	$< 20 \mu\text{s}$
Trigger modes	Software, hardware, continuous
Optical head dimensions	$\varnothing 15 \text{ mm} \times 30 \text{ mm}$
Optical head weight	20 g
Detector dimensions	$\varnothing 52 \text{ mm} \times 10 \text{ mm}$
Detector weight	25 g

tation error will exceed the resolution limit of the system if the misalignment is greater than 0.02° . By careful mounting, these errors can be minimized.

The system properties are gathered in Table 1. It must be noted that the measurement range, now equal to $\pm 300 \mu\text{m}$ could optionally be adjusted simply by changing the beam diameter. By increasing it, the range is correspondingly expanded, provided that the beam diameter remains smaller than the detector radius. Doing so, however, also proportionally reduces the positional resolution and accuracy.

4. Conclusion

An optical measuring system, capable of direct measuring of two translational degrees of freedom was presented, suitable specifically for measuring deformations in mechanical components. The system is composed of optical head producing a stable reference beam, and a detector board with digital interface. The system was calibrated and the resulting accuracy was found to be adequate for applications in precision systems. The verified value of resolution is at least $0.1 \mu\text{m}$ and the error distribution shows a standard deviation of $0.4 \mu\text{m}$. Stability tests in temperature-controlled environment indicate positional drift under $2 \mu\text{m}$ in 10 h in both DOF. Real-time static and dynamic measurements with sampling rates up to 1.2 kHz are possible. Multiple laser-detector sets can be connected to a single master board, thus measuring arbitrary number of DOF in a flexible mechanical system. The fact that the only necessary components in the affected structure are the modestly dimensioned optical head and detector unit, makes the integration of the system feasible in existing and future machinery. Being under the focus of commercial partners, a number of industrial applications is emerging.

Acknowledgements

The authors wish to acknowledge the assistance of Boštjan Batagelj (University of Ljubljana), Primož Kušar (Jožef Stefan Institute) and members of Institute of Production Engineering, TU Graz.

References

- [1] Sohn YJ, Kwon JH, Choe OS. Portable autocollimators using the laser diode and the position sensitive detector. *Rev Sci Instrum* 1998;69:402–5.
- [2] Armstrong TR, Fitzgerald MP. An autocollimator based on the laser head of a compact disc player. *Measur Sci Technol* 1992;3:1072–6.
- [3] Fan KC, Chu CL, Liao JL, Mou JI. Development of a high precision straightness measuring system with DVD pick-up head. *Measur Sci Technol* 2003;14:47–54.
- [4] Kovač I, Frank A. Testing and calibration of coordinate measuring arms. *Precis Eng* 2001;25:90–9.
- [5] Huang PS, Ni J. On-line error compensation of coordinate measuring machines. *Int J Mach Tools Manuf* 1995;35:725–38.
- [6] Feng Q. A straightness measurement system using a single-mode fiber-coupled laser module. *Optics Laser Technol* 2004;36:279–83.
- [7] Fan KC, Zhao Y. A laser straightness measurement system using optical fiber and modulation techniques. *Int J Mach Tools Manuf* 2000;40:2073–81.

- 414 [8] Kuang C, Feng Q, Zhang B, Liu B, Chen S, Zhang Z. A four-degree-of-
415 freedom laser measurement system (FDMS) using a single-mode fiber-
416 coupled laser module. *Sens Actuators A: Phys* 2005;125:100–8. 423
- 417 [9] Golnabi H. Linearity in output signal of optical position-sensing detector
418 systems. *Optics Laser Technol* 2000;32:311–6. 424
- 419 [10] Deemester F, Van Brussel H. Real-time optical measurement of robot struc-
420 tural deflections. *Mechatronics* 1991;1:73–86. 425
- 421 [11] Xu WL, Tso SK. Sensor-based deflection modelling and compensation
422 control of flexible robotic manipulator. *Mech Mach Theory* 1998;33:
909–24. 426
- [12] Yang TW. Dynamic modeling based on real-time deflection measurement
and compensation control for flexible multi-link manipulators. *Dynam*
Control 2001;11:5–24. 427
- [13] Tso SK, Yang TW, Xu WL, Sun ZQ. Vibration control for a flexible-
link robot arm with deflection feedback. *Int J Non-Linear Mech* 2003;38:
51–62. 428
- [14] Beitz W, Kuttner KH. *Dubbel handbook of mechanical engineering*; 1994. 429
- [15] Hirn C. Entwicklung eines klimatisierten Präzisionskomparators für
Längen und Geradheitsmessungen bis 5 Meter, *Technik report* 19, no. 6,
1992. p. 23–6 [in German]. 430
431
432

UNCORRECTED PROOF